High optical performance of blue-emissive $CsPbBr_3$ perovskite quantum dots embedded in molecular organogels

Marta Vallés-Pelarda, Andrés F. Gualdrón-Reyes, Carles Felip-León, César A. Angulo-Pachón, Said Agouram, Vicente Muñoz-Sanjosé, Juan F. Miravet, Francisco Galindo*, Iván Mora-Seró**

M. Vallés-Pelarda, Dr. A. F. Gualdrón-Reyes, Prof. I. Mora-Seró
Institute of Advanced Materials (INAM), University Jaume I. Av. de Vicent Sos Baynat, s/n 12006, Castelló de la Plana, Spain.
E-mail: sero@uji.es

Dr. C. Felip-León, Dr. C. A. Angulo-Pachón, Prof. Juan F. Miravet, Prof. Francisco Galindo
Department of Inorganic and Organic Chemistry, University Jaume I, Av. de Vicent Sos Baynat, s/n 12006, Castelló de la Plana, Spain.
E-mail: francisco.galindo@uji.es, miravet@uji.es

Dr. S. Agouram, Prof. V.Muñoz-Sanjosé
Department of Applied Physics and Electromagnetism, University of Valencia, 46100 Valencia, Spain.

Prof. I. Mora-Seró, Dr. S. Agouram, Prof. V. Muñoz-Sanjosé
Materials for Renewable Energy (MAER), Unitat Mixta d'Investigació UV-UJI

Keywords: perovskite quantum dots, organogels, blue emission, photoluminescence quantum yield

Abstract

Perovskite quantum dots (PQDs) have fascinating optoelectronic properties, such as high photoluminescence quantum yield (PLQY) for a broad range of materials and the possibility of obtaining different band-gaps with the same material or halide combinations. Nevertheless, blue-emissive materials generally present limited PLQY or color stability. Here, two molecular organogels based on a derivative of an aminoacid and succinic acid with embedded $CsPbBr_3$ quantum dots are studied, the obtained green and blue emission is analyzed. TEM

and SAED measurements were performed to confirm that there was no significant change in the average size of the PQDs or in the crystal structure. High photoluminescence quantum yield (PLQY), almost 100%, was achieved for blue emission. This contribution opens the door to achieve a post-synthetic treatment for synthesizing blue-emissive PNCs with high optical performance, which can be attractive for optoelectronic applications.

1. Introduction

Perovskite quantum dots (PQDs) have been widely studied due to their exceptional properties, such as high photoluminescence with narrow emission peaks and high absorption coefficient. In addition, their band-gap can be easily tuned by changing their chemical composition (different halides or mixtures) or varying the morphology of the nanoparticles (NPs) (from quantum dots to nanoplatelets).[1–4] All of these properties make them suitable for many different applications: optoelectronic devices, lasers, scintillators, sensors. [5–10]

Although the emission wavelength of these NPs can be tuned from UV to near IR, the achievement of a high photoluminescence quantum yield (PLQY) in blue emissive PQDs is still challenging. The inorganic perovskite emitting in the blue region is the one with high content of chloride ($CsPbCl_3$) and they have relatively low PLQY. One strategy to increase the PLQY of these PQDs is a mixture of halides (Br/Cl), however, these materials could show phase segregation and color instability.[11] Consequently, other approaches attending to optimizing synthetic protocols have been successfully studied.[12] Recently, 70% PLQY was reported for $CsPbBr_3$ nanoplatelets, in films 88% with quasi-2D perovskites and almost unity PLQY was reported doping with $CdCl_2$ the pure chloride perovskite.[1,10,13] A high PLQY was also achieved by doping $CsPbBr_3$ nanocrystals (NCs) with neodymium (III).[14]

On the other hand, previous reports have incorporated NPs inside a gel matrix, showing different effects such as an enhancement of the PL emission, a small redshift in the emission wavelength or even anion exchange reactions of perovskite PQDs that take place inside.[15–18] However, only variations around 0.3 eV in the band gap were reported when changing the capping ligand of different NPs.[19,20] A recent work reported a blueshift in the emission of $CsPbBr_3$ QDs after a ligand exchange and the blueshift was explained by a reduction of the particle size.[21]

In this work, a mixture of PQDs and organogelator molecules will be presented, showing a change in their optical properties, specially band gap and PLQY. A shift in the emission from green to blue was observed. After the gel formation, $CsPbBr_3$ QDs were embedded in the gel matrix showing different emission wavelengths, green or blue, depending on the organogelator structure. In addition, an increase in the PLQY was achieved for blue emission up to almost 100%, keeping around 80% of the initial value after 4 months. The combination of organic gels and PQDs can be useful to improve the photophysical properties of NPs, which can increase their interest in the optoelectronic field.

2. Results and discussion

The molecular organogelators here studied are derivatives of an amino acid and succinic acid. This type of compounds forms fibrillar structures after a heating/cooling procedure, as described in the Experimental Section. The difference between them is the aliphatic chain arrangement of a radical; one is a linear hexyl radical (Hx), while the other is a cyclohexyl radical (Chx) (see **Figure 1a)**.[22] This small difference has shown to have a strong influence on the QD properties after the gel formation.

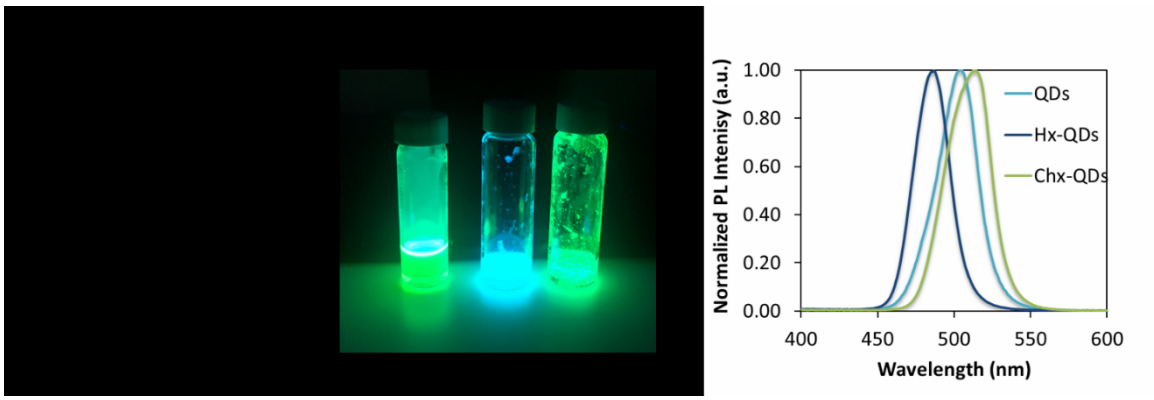

Figure 1. a) Chemical structure of the two different organogelators, Hx and Chx. b) Picture of the QDs solution (left), Hx-QDs (center) and Chx-QDs (right) under UV light. c) Normalized PL spectra of the different samples: $CsPbBr_3$ solution (light blue), Hx matrix with $CsPbBr_3$ QDs (dark blue) and CHx matrix with $CsPbBr_3$ QDs (green).

Comparing these organic molecules with the ligands surrounding the QDs (oleylamine and oleic acid), they have similar functional groups. The gelator with the cyclohexyl moiety preserves the properties of the $CsPbBr_3$ QDs, the emission is green. However, when the chain is linear, it shows a blue emission. In **Figure 1b**, both gel matrixes are shown under UV light and the different behavior is observed. As mentioned before, the solutions need to be heated in order to obtain the different gels. For that reason, the effect of the temperature was first studied. A PQDs solution was heated following the procedure to form the gel and it was characterized by TEM, see **Figure S1**. The formation of some big NPs is observed, increasing the average size by around 1 nm, which could be attributed to the Ostwald ripening process.[23,24] In addition, the effect on the PLQY was also analyzed. Although first measurements after the treatment of the NPs usually showed a decrease in the quantum yield, over the time, it was recovered almost completely.

Figure 1c shows the normalized PL spectra of the QDs solution and the QDs embedded in the different organogels. Taking as reference the emission wavelength of the QDs in solution at

507 nm, a small redshift of approximately 7 nm is observed for the Chx matrix (Chx-QDs), while a blueshift of around 20 nm is observed in the Hx matrix (Hx-QDs). The full width at half maximum (FWHM) of the PL peaks are 29 nm for the QDs solution, 26 nm for the Hx-QDs and 35 nm for the Chx-QDs. Different heating temperatures were used, analyzing the effect on the emission in the Hx-QDs. In **Table S1**, a comparison of the emission wavelength with these temperatures is shown. As mentioned before, it has been reported the use of aminoacids such as α-amino butyric acid after the synthesis of $CsPbBr_3$ PQDs, and the impact on their photophysical properties.[21] Because of the bi-functional structure of the α-amino butyric acid, ligand exchange with conventional oleylamine and oleic acid is performed, causing a better surface passivation, and thereby the enhacement of the optical features. This fact includes a blue-sfhit in the PL peak, indication of the surface modification with a short-capping ligand, also mediating the decrease of QDs size. Interestingly, the opposite effect observed for Chx, despite the similar structure to Hx, allows to suggest that an efficient surface coverage is hindered. In order to explain this difference, it must be recalled that Hx and Chx self-associate in a very different manner, as it was demonstrated in the past: whereas the molecular architecture of Chx enables for an efficient self-assembly and packing into fibres, Hx is less prone to self-associate. This phenomenon is attributed to entropic factors and in the materials here under study it would imply that molecules of Hx could be more available to participate in the passivation process than molecules of Chx.[22]

Size, morphology and elemental composition of the Hx-QDs and Chx-QDs samples were characterized by high-resolution transmission electron microscopy (HRTEM), selected area electron diffraction (SAED) and energy-dispersive X-ray spectroscopy (EDX). TEM of PQDs in solution is plotted in **Figure 2a**. From TEM images in **Figure 2b-c**, an arrangement of PQDs following the fibers is observed for Hx-QDs and Chx-QDs samples. For $CsPbBr_3$ QDs in solution and in the Hx matrix, the size is similar, being the average size 8.7 and 8.3 nm,

respectively (see **Figure S2**). However, a clear difference in the particle size is observed for the $CsPbBr_3$ QDs in Chx matrix, with an average size of 14 nm. The increase of QDs size in presence of Chx induces the redshift in the PL emission discussed above, while the blueshift in the PL peak of the Hx-QDs sample cannot be explained by a decrease in the size of the QDs.[21,25] In addition, SAED patterns in **Figure 2d-f** do not show a change in the crystal structure, which, according to previous works, is orthorhombic *Pnma*. [26–28] From the HRTEM, the *d* values obtained for QDs, Hx-QDs and Chx-QDs are 0.29, 0.59 and 0.29 nm and could be attributed to (2 0 2), (0 2 0) and (2 0 2) family planes, respectively, which agree with the orthorhombic phase (ICSD 231019).[28] At this point, we deduced that organogelators do not induce changes in the crystal structure of the PQDs.

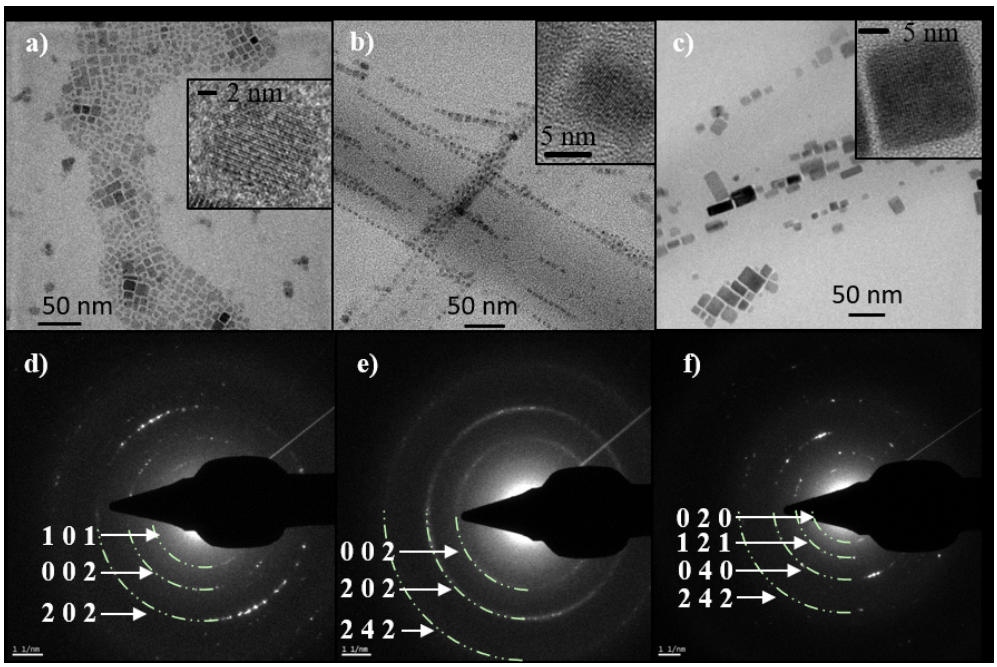

Figure 2 a) and d) TEM image and SAED patterns of the PQDs solution. b) and e) TEM image and SAED patterns of the Hx-QDs gel. c) and f) TEM image and SAED patterns of the Chx-QDs gel. Insets in the TEM images are HRTEM images.

Fourier transformed infrared spectroscopy (FTIR) was employed to obtain information about the ligands covering the PQDs surface. In **Figure 3a**, three samples are shown: the $CsPbBr_3$ QDs solution, the Hx gel and the Hx-QDs. A comparison between Chx and Chx-QDs samples is also shown in **Figure 3b**. From the $CsPbBr_3$ PQDs solution, the signals in the range of 2852-2956 cm^{-1} and 1465 cm^{-1} correspond to the presence of oleic acid (OA) and oleylamine (OLA) covering the PQD surface. These bands are associated to the C-H stretching and the C-H bending, respectively. The broad band starting at 3300 cm^{-1} is associated to the O-H stretching and a band at 1715 cm^{-1} from the C=O stretching of the carboxylic acid. Also, the bands observed at 1534 and 1406 cm^{-1} are associated to the O-C-O stretching.[29,30] **Figure S3** shows the typical FTIR of OA and OLA, where their corresponding peaks match with those of the PQDs, corroborating thus the above discussed assignment of the bands. Then, in the Hx gel spectrum, the most significant bands appear at 3283 cm^{-1} from N-H stretching, 1697 cm^{-1} from C=O (carboxylic group) and from the amides at 1632 and 1540 cm^{-1}. [9,29] In the Hx-QDs spectrum, the peaks match the ones in the reference samples with slight variations in the position. Comparing these three samples, a decrease in the relative intensity of the assigned band at 1697 cm^{-1} in the Hx spectrum is observed when the QDs are present, which may suggest that there is an interaction that reduces the C=O vibrational mode. However, by comparing the FTIR spectra of Chx and Chx-QDs samples, there is no significant variation in the relative intensity of any band.[9] At this stage, we could conclude that Hx shows a high influence on the surface properties of $CsPbBr_3$ PQDs compared with Chx organic ligand, which does not seem suffer any alteration after interact with the perovskite colloidal solution. This observation would corroborate that Chx is more prone to self-associate due to the preorganization of its molecular structure, whereas Hx, less preorganized, is more available for the interaction with the surface of the perovskite.

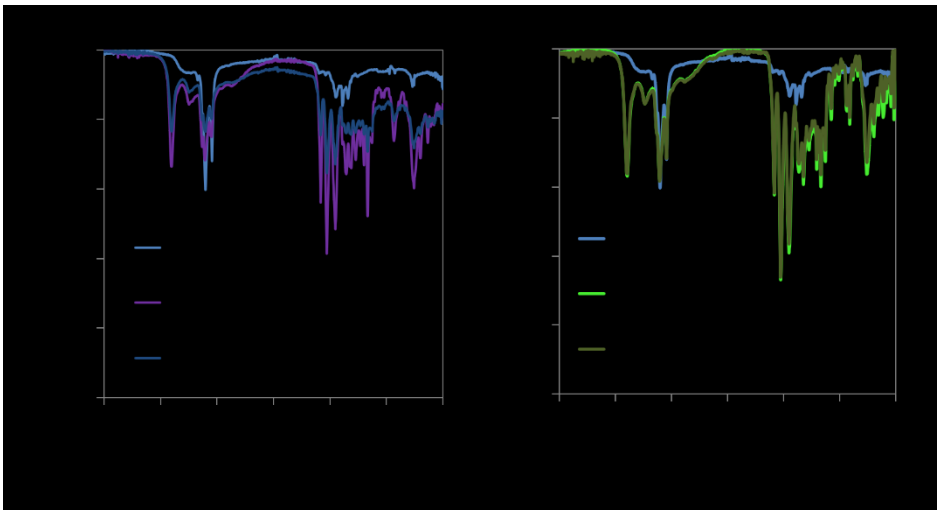

Figure 3. a) FTIR spectra of $CsPbBr_3$ QDs in solution (light blue), Hx gel matrix (purple) and Hx with embedded QDs (dark blue). b) FTIR spectra of $CsPbBr_3$ QDs in solution (light blue), Chx gel matrix (green) and Chx with embedded QDs (dark green).

The stability of $CsPbBr_3$ PQDs has been also studied under ambient conditions in presence of the organogelators. By measuring the photoluminescence quantum yield of the materials, $CsPbBr_3$ QDs solution displays a value around 32% after one purification. After adding the gelators and forming the gel, Hx-QDs sample showed a huge improvement PLQY with values arriving to 95%, while Chx-QDs one was 70%. As shown in **Figure 4**, these modified PQDs have a relatively high PLQY along 4 months. The emission peak of the Hx sample shows a blue-shift along the time, starting at 490 nm and moving to 480 nm. Chx emission peak remains around 517 nm. Considering that the PLQY of the $CsPbBr_3$ PQDs was increased in presence of the organogelators, we presume that these aminoacid derivatives enhance the passivation of surface defects from PQDs, mitigating the non-radiative recombination pathway. Hence, the radiative channel is facilitated, providing a higher PLQY. Then, the materials can be stable for a long-term, preserving their intrinsic properties. Nevertheless, the fact that PQDs can reach the 99% PLQY can suggest that the ability for surface coverage from Hx is better than Chx, as a result of a linear hexyl chain radical. Therefore, we

concluded that Hx and Chx can be used as efficient surface ligand passivators during the post-synthetic treatment of $CsPbBr_3$ PQDs, which increases the quality of the materials and their stability.

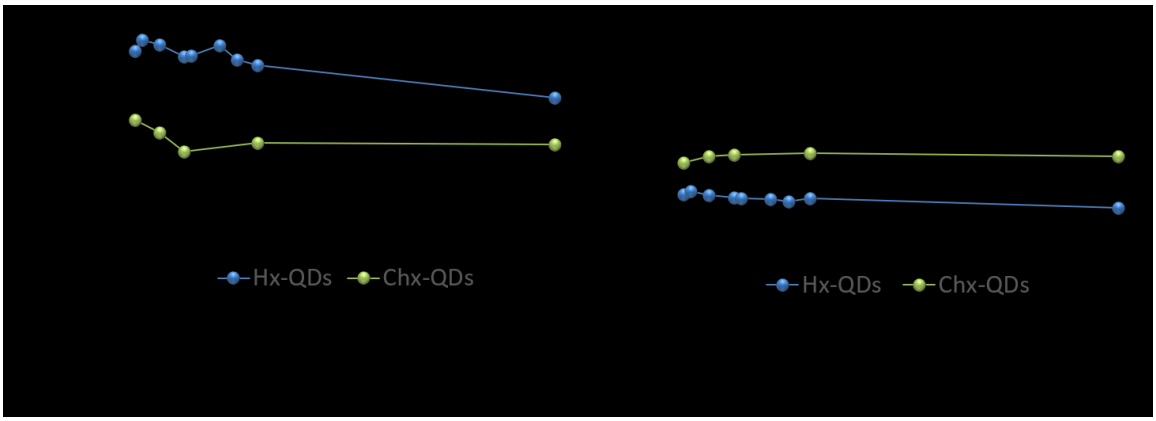

Figure 4. Evolution of a) the PLQY and b) the emission wavelength of both gel matrixes: Hx (blue) and Chx (green).

3. Summary and Conclusions

This study has successfully prepared two different organogels with embedded $CsPbBr_3$ perovskite quantum dots, Hx-QDs and Chx-QDs. The difference in the structure of these organogelators show an effect on the PQDs, varying the emission from green to blue in the case of Hx gel. In addition to this effect, the PLQY increases in both cases, which points to an interaction between the organogels and the surface of the QDs as shows the FTIR spectra. In the case of Hx, this short-chain aminoacid derivative can passivate efficiently the PQDs surface due to a lower self-assembled ability than the Chx. Hence, a 99% PLQY can be achieved, with a long-term stability. For Chx, the cyclohexyl radical can produce a better fiber network, hindering ligand passivation and generating a lower improvement in the photophysical features of the PQDs, while original green emission is slightly redshifted due to QD size increase. The use of both kind of organogelators based on aminoacids is a potential

post-synthetic approach to improve the quality of PQDs, which can be widely useful for optoelectronics.

4. Experimental Section

Synthesis of $CsPbBr_3$ QDs: $CsPbBr_3$ QDs synthesis and purification were based on previously reported methods.[3,31] For the Cs-oleate solution, 0.618 g Cs_2CO_3 (Sigma-Aldrich, 99.9 %), 1.9 mL OA (Sigma Aldrich, 90 %) and 30 mL of 1-octadecene (ODE, Sigma-Aldrich, 90 %) were kept under continuous stirring under vacuum at 80 ºC and 120 °C 30 min each. Then, the solution was heated at 140 °C in nitrogen atmosphere until the Cs_2CO_3 was completely dissolved and, after that, it was kept at 120 °C.

1.0 g $PbBr_2$ (ABCR, 99.999 %) in 50 mL ODE was heated at 120 ºC under continuous stirring and kept 1 h at this temperature under vacuum. Then, under N_2, 5 mL OA and 5 mL OLA (Sigma-Aldrich, 98 %) were added to the flask and the solution was heated to 175 °C, injecting quickly 4 mL Cs-oleate solution and after 5 s the reaction was quenched by cooling down the reaction in an ice bath.

$CsPbBr_3$ QDs were isolated and purified by adding 60 mL of methyl acetate and centrifuging the mixture at 4700 rpm 5 min. The precipitated QDs where dispersed in hexane (Honeywell, 99.7%). To obtain the desired concentration, the QDs solution was dried and re-dispersed in toluene for a final concentration 50 mg mL^{-1}.

Preparation of the gels: Syntheses of Hx and Chx were based on a previous report.[22] The different gelators were weighed to obtain a 2.5 mg mL^{-1} solution in toluene for Hx and 2.0 mg mL^{-1} for Chx. To form the gel matrix, they were heated with an air gun and let it cool down. When they were completely formed, the perovskite QDs were added to obtain a final concentration of 1 mg mL^{-1} and the gels were heated and cooled again.

Characterization: PL and PLQY measurements were carried out using an absolute quantum yield spectrometer (C9920-02, Hamamatsu), with a Xe lamp (150 W) as light source. Samples were excited at 350 nm. Transmission Electron Microscopy (TEM) measurements were carried out in a field emission gun TECNAI G^2 F20 microscope operated at 200 kV. UV-visible absorption spectra were measured by a PerkinElmer LAMBDA 1050+ UV/Vis/NIR spectrophotometer. FTIR spectroscopy was measured using a FTIR spectrometer FT/IR-6200 (Jasco) in ATR using a diamond glass.

Supporting Information
Supporting Information is available from the Wiley Online Library or from the author.

Acknowledgements

M.V.-P. A. G.-R. and I.M.-S. acknowledge the support of the European Research Council (ERC) via Consolidator Grant (724424 - No-LIMIT) and Generalitat Valenciana via Prometeo Grant Q-Devices (Prometeo/2018/098). M. V-P. acknowledges Universitat Jaume I for the support through FPI Fellowship Program (PREDOC/2017/40). F.G. and J. F. M. acknowledge the support of Spanish Ministerio de Ciencia, Innovación y Universidades (RTI2018-101675-B-I00). S.A. and V.M.-S. acknowledge the support of the EU (FEDER) and MINECO under project TEC2017-85912-C2-2. We acknowledge SCIC from UJI for help with FTIR characterization.

Received: ((will be filled in by the editorial staff))
Revised: ((will be filled in by the editorial staff))
Published online: ((will be filled in by the editorial staff))

References

[1] B. J. Bohn, Y. Tong, M. Gramlich, M. L. Lai, M. Döblinger, K. Wang, R. L. Z. Hoye, P. Müller-Buschbaum, S. D. Stranks, A. S. Urban, L. Polavarapu, J. Feldmann, *Nano Lett.* **2018**, *18*, 5231.

[2] Q. Van Le, K. Hong, H. W. Jang, S. Y. Kim, *Adv. Electron. Mater.* **2018**, *4*, 1800335.

[3] L. Protesescu, S. Yakunin, M. I. Bodnarchuk, F. Krieg, R. Caputo, C. H. Hendon, R. X. Yang, A. Walsh, M. V Kovalenko, *Nano Lett.* **2015**, *15*, 3692.

[4] A. Dutta, S. K. Dutta, S. Das Adhikari, N. Pradhan, *ACS Energy Lett.* **2018**, *3*, 329.

[5] S. Huang, M. Guo, J. Tan, Y. Geng, J. Wu, Y. Tang, C. Su, C. C. Lin, Y. Liang, *ACS Appl. Mater. Interfaces* **2018**, *10*, 39056.

[6] C.-Y. Huang, C. Zou, C. Mao, K. L. Corp, Y.-C. Yao, Y.-J. Lee, C. W. Schlenker, A. K. Y. Jen, L. Y. Lin, *ACS Photonics* **2017**, *4*, 2281.

[7] Y. Wang, X. Li, J. Song, L. Xiao, H. Zeng, H. Sun, *Adv. Mater.* **2015**, *27*, 7101.

[8] F. Zhou, Z. Li, W. Lan, Q. Wang, L. Ding, Z. Jin, *Small Methods* **2020**, *n/a*, 2000506.

[9] M. Fang, S. Huang, D. Li, C. Jiang, P. Tian, H. Lin, C. Luo, W. Yu, H. Peng, *Nanophotonics* **n.d.**, *7*, 1949.

[10] J. Xing, Y. Zhao, M. Askerka, L. N. Quan, X. Gong, W. Zhao, J. Zhao, H. Tan, G. Long, L. Gao, Z. Yang, O. Voznyy, J. Tang, Z.-H. Lu, Q. Xiong, E. H. Sargent, *Nat. Commun.* **2018**, *9*, 3541.

[11] N. K. Kumawat, X.-K. Liu, D. Kabra, F. Gao, *Nanoscale* **2019**, *11*, 2109.

[12] A. Dutta, R. K. Behera, P. Pal, S. Baitalik, N. Pradhan, *Angew. Chemie Int. Ed.* **2019**, *58*, 5552.

[13] N. Mondal, A. De, A. Samanta, *ACS Energy Lett.* **2019**, *4*, 32.

[14] Y. Xie, B. Peng, I. Bravić, Y. Yu, Y. Dong, R. Liang, Q. Ou, B. Monserrat, S. Zhang, *Adv. Sci.* **2020**, *n/a*, 2001698.

[15] P. D. Wadhavane, R. E. Galian, M. A. Izquierdo, J. Aguilera-Sigalat, F. Galindo, L. Schmidt, M. I. Burguete, J. Pérez-Prieto, S. V Luis, *J. Am. Chem. Soc.* **2012**, *134*, 20554.

[16] W. J. Peveler, J. C. Bear, P. Southern, I. P. Parkin, *Chem. Commun.* **2014**, *50*, 14418.

[17] J.-M. Park, J. Park, Y.-H. Kim, H. Zhou, Y. Lee, S. H. Jo, J. Ma, T.-W. Lee, J.-Y. Sun,

Nat. Commun. **2020**, *11*, 4638.

[18] M. Yamauchi, Y. Fujiwara, S. Masuo, *ACS Omega* **2020**, *5*, 14370.

[19] R. Nadler, J. F. Sanz, *J. Phys. Chem. A* **2015**, *119*, 1218.

[20] J. Amaya Suárez, J. J. Plata, A. M. Márquez, J. Fernández Sanz, *J. Phys. Chem. A* **2017**, *121*, 7290.

[21] S. R, H. V Vishaka, K. J, R. G. Balakrishna, *ACS Appl. Nano Mater.* **2020**, *3*, 6089.

[22] C. A. Angulo-Pachón, C. Gascó-Catalán, J. J. Ojeda-Flores, J. F. Miravet, *ChemPhysChem* **2016**, *17*, 2008.

[23] J. B. Hoffman, G. Zaiats, I. Wappes, P. V Kamat, *Chem. Mater.* **2017**, *29*, 9767.

[24] Y. De Smet, L. Deriemaeker, R. Finsy, *Langmuir* **1997**, *13*, 6884.

[25] F. Bertolotti, G. Nedelcu, A. Vivani, A. Cervellino, N. Masciocchi, A. Guagliardi, M. V Kovalenko, *ACS Nano* **2019**, *13*, 14294.

[26] P. Cottingham, R. L. Brutchey, *Chem. Commun.* **2016**, *52*, 5246.

[27] M. C. Brennan, M. Kuno, S. Rouvimov, *Inorg. Chem.* **2019**, *58*, 1555.

[28] P. Cottingham, R. L. Brutchey, *Chem. Mater.* **2018**, *30*, 6711.

[29] J. Pan, L. N. Quan, Y. Zhao, W. Peng, B. Murali, S. P. Sarmah, M. Yuan, L. Sinatra, N. M. Alyami, J. Liu, E. Yassitepe, Z. Yang, O. Voznyy, R. Comin, M. N. Hedhili, O. F. Mohammed, Z. H. Lu, D. H. Kim, E. H. Sargent, O. M. Bakr, *Adv. Mater.* **2016**, *28*, 8718.

[30] L. C. Cass, M. Malicki, E. A. Weiss, *Anal. Chem.* **2013**, *85*, 6974.

[31] A. Swarnkar, A. R. Marshall, E. M. Sanehira, B. D. Chernomordik, D. T. Moore, J. A. Christians, T. Chakrabarti, J. M. Luther, *Science (80-.).* **2016**, *354*, 92 LP.

Marta Vallés-Pelarda, Andrés F. Gualdrón-Reyes, Carles Felip-León, César A. Angulo-Pachón, Said Agouram, Vicente Muñoz-Sanjosé, Juan F. Miravet*, Francisco Galindo*, Iván Mora-Seró*

High optical performance of blue-emissive $CsPbBr_3$ perovskite quantum dots embedded in molecular organogels

ToC figure

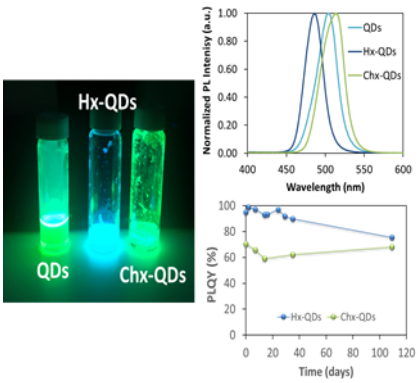

$CsPbBr_3$ perovskite quantum dots are embedded in two different organogels, Hx and Chx. Both short-chain capping ligands improve the photophysical properties of PQDs, being more significative by using the hexyl-radical aminoacid derivative. In this case, a 99% PLQY with blue emission and long-term stability is achieved, considering this post-synthetic treatment attractive for enhancing the quality of blue-emissive PQDs.

Supporting Information

High optical performance of blue-emissive $CsPbBr_3$ perovskite quantum dots embedded in molecular organogels

Marta Vallés-Pelarda, Andrés F. Gualdrón-Reyes, Carles Felip-León, César A. Angulo-Pachón, Said Agouram, Vicente Muñoz-Sanjosé, Juan F. Miravet, Francisco Galindo*, Iván Mora-Seró**

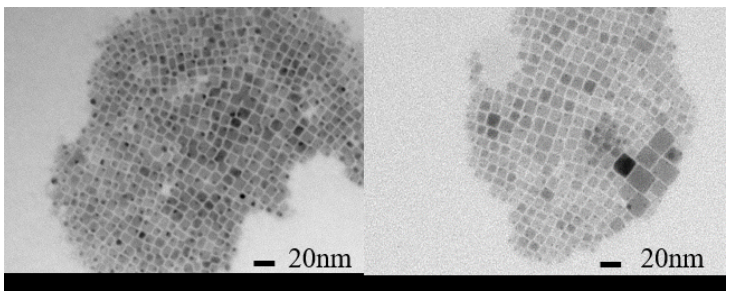

Figure S1. TEM images of QDs solution as prepared (left) and heated (right).

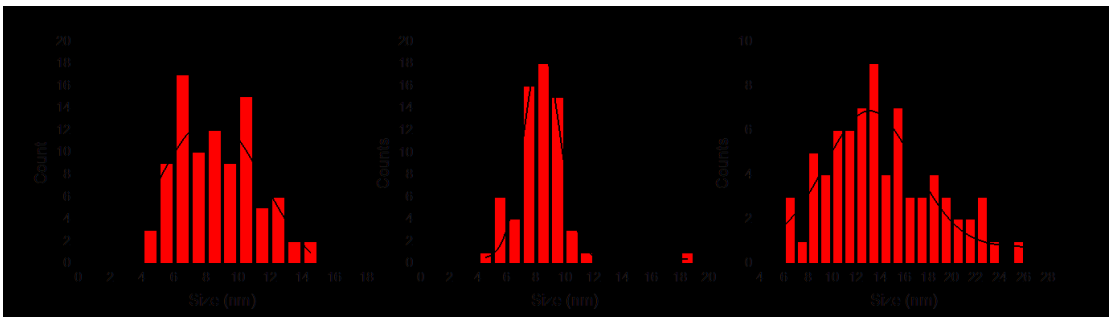

Figure S2. a), b) and c) Size distribution histograms of $CsPbBr_3$ QDs solution, QDs embedded in Hx and Chx, respectively.

Table S1. Characterization of Hx-QDs samples prepared at different temperatures.

Conditions	λ (nm)	PLQY (%)
QD solution	516	49
200ºC	466	75
220ºC	471	77
240ºC	471	71

Table S2. Energy Dispersive X-Ray analysis. Atomic %

	Cs (%)	Pb(%)	Br(%)
$CsPbBr_3$ QDs	36.3±2.3	27±3	37±5
Hx + $CsPbBr_3$ QDs	32.6±1.1	25.7±2.4	41.7±1.8
Chx + $CsPbBr_3$ QDs	30±3	23.6±0.7	47±3

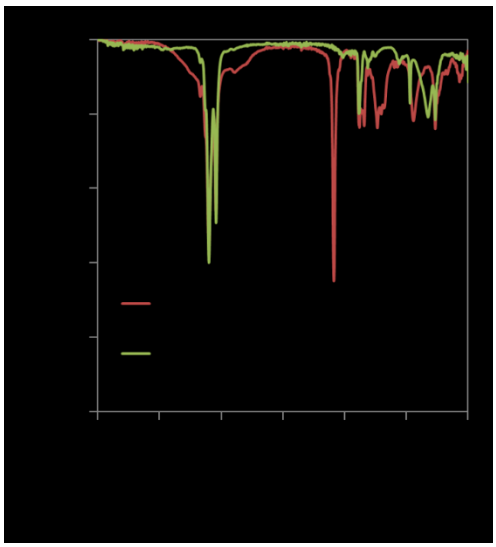

Figure S3. FTIR spectra of oleic acid and oleylamine capping ligands used for conventional CsPbBr3 QDs synthesis.